SIMPLE GENERAL FORMULAE FOR SAND TRANSPORT IN RIVERS, ESTUARIES AND COASTAL WATERS

by L.C. van Rijn (www.leovanrijn-sediment.com)

1. General characteristics

Sand can be transported by gravity-, wind-, wave-, tide- and density-driven currents (current-related transport), by the oscillatory water motion itself (wave-related transport) as caused by the deformation of short waves under the influence of decreasing water depth (wave asymmetry) or by a combination of currents and short waves.
In rivers the gravity-induced flow generally is steady or quasi-steady generating bed load and suspended load transport of particles in conditions with an alluvial river bed. A typical feature of sediment transport along an alluvial bed is the generation of bed forms from small-scale ripples (order 0.1 m) up to large-scale dunes (order 100 m). The adjustment of large-scale bed forms such as dunes and sand waves may lead to non-steady effects (hysteresis effects) as it takes time for these large-scale features to adjust to changed flow conditions (flood waves).
In the lower reaches of the river (estuary or tidal river) the influence of the tidal motion may be become noticeable introducing non-steady effects with varying current velocities and water levels on a diurnal or semi-diurnal time scale. Furthermore, density-induced flow may be generated due to the interaction of fresh river water and saline sea water (salt wedge).
In coastal waters the sediment transport processes are strongly affected by the high-frequency waves introducing oscillatory motions acting on the particles. The high-frequency (short) waves generally act as sediment stirring agents; the sediments are then transported by the mean current.
Field experience over a long period of time in the coastal zone has led to the notion that storm waves cause sediments to move offshore while fair-weather waves and swell return the sediments shorewards. During conditions with low non-breaking waves, onshore-directed transport processes related to wave-asymmetry and wave-induced streaming are dominant, usually resulting in accretion processes in the beach zone. During high-energy conditions with breaking waves (storm cycles), the beach and dune zone of the coast are attacked severely by the incoming waves, usually resulting in erosion processes.

2. Definitions

Sand transport is herein defined as the transport of particles with sizes in the range of 0.05 to 2 mm as found in the bed of rivers, estuaries and coastal waters. The two main modes of sand transport are bed-load transport and suspended load transport. The bed-load transport is defined to consist of gliding, rolling and saltating particles in close contact with the bed and is dominated by flow-induced drag forces and by gravity forces acting on the particles. The suspended load transport is the irregular motion of the particles through the water column induced by turbulence-induced drag forces on the particles. Detailed information is presented by **Van Rijn (1993)**.
The definition of bed-load transport is not universally agreed upon. Sheet flow transport at high bed-shear stresses may be considered as a type of bed-load transport, but it may also be seen as suspended load transport. Some regard bed-load transport as occurring in the region where concentrations are so high that grain-grain interactions are important, and grains are not supported purely by fluid forces.
The suspended load transport can be determined by depth-integration of the product of sand concentration and fluid velocity from the top of the bed-load layer to the water surface.
Herein, the net (averaged over the wave period) total sediment transport in coastal waters is defined as the vectorial sum of net the bed load (q_b) and net suspended load (q_s) transport rates: $q_{tot} = q_b + q_s$.
For practical reasons the suspended transport in coastal waters will be subdivided into current-related and wave-related transport components.

Thus, the suspended sand transport is represented as the vectorial sum of the current-related ($q_{s,c}$ in current direction) and the wave-related ($q_{s,w}$ in wave direction) transport components, as follows:

$$q_s = q_{s,c} + q_{s,w} = \int vc\, dz + \int <(V-v)(C-c)> dz \qquad (1)$$

in which:
$q_{s,c}$ = time-averaged current-related suspended sediment transport rate and
$q_{s,w}$ = time-averaged wave-related suspended sediment transport rate (oscillating component),
v= time-averaged velocity,
V= instantaneous velocity,
C= instantaneous concentration and c= time-averaged concentration,
<…> represents averaging over time,
∫.. represents the integral from the top of the bed-load layer to the water surface.

The precise definition of the lower limit of integration is of essential importance for accurate determination of the suspended transport rates. Furthermore, the velocity and concentration profiles must be known.

The current-related suspended transport component ($q_{s,c}$) is defined as the advective transport of sediment particles by the time-averaged (mean) current velocities (longshore currents, rip currents, undertow currents); this component therefore represents the transport of sediment carried by the steady flow.
In the case of waves superimposed on the current both the current velocities and the sediment concentrations will be affected by the wave motion. It is known that the wave motion reduces the current velocities near the bed while, in contrast, the near-bed concentrations are strongly increased due to the stirring action of the waves. These effects are included in the current-related transport.
The wave-related suspended sediment transport ($q_{s,w}$) is defined as the transport of sediment particles by the high-frequency and low-frequency oscillating fluid components (cross-shore orbital motion).
The suspended transport vector can be combined with the bed load transport vector to obtain the total transport vector: q_{tot}.

In this note only the current-related bed load and suspended load transport components are considered. Usually, these components are dominant in river and tidal flows and also in wave-driven longshore flows.

3. Sand transport in steady river flow

3.1 Basic characteristics

The transport of bed material particles may be in the form of either bed-load or bed-load plus suspended load, depending on the size of the bed material particles and the flow conditions. The suspended load may also contain some wash load (usually, clay and silt particles smaller than 0.05 mm), which is generally defined as that portion of the suspended load which is governed by the upstream supply rate and not by the composition and properties of the bed material. The wash load is mainly determined by land surface erosion (rainfall, no vegetation) and not by channel bed erosion. Although in natural conditions there is no sharp division between the bed-load transport and the suspended load transport, it is necessary to define a layer with bed-load transport for mathematical representation.

When the value of the bed-shear velocity just exceeds the critical value for initiation of motion, the particles will be rolling and sliding or both, in continuous contact with the bed. For increasing values of the bed-shear velocity, the particles will be moving along the bed by more or less regular jumps, which are called saltations. When the value of the bed-shear velocity exceeds the fall velocity of the particles, the sediment particles can be lifted to a level at which the upward turbulent forces will be comparable with or of higher order than the submerged weight of the particles and as result the particles may go in suspension.

The sediment transport in a steady uniform current over an alluvial bed is assumed to be equal to the transport capacity defined as the quantity of sediment that can be carried by the flow without net erosion or deposition, given sufficient availability of bed material (no armour layer).
In general, a river flood wave is a relatively slow process with a time scale of a few days. Consequently, the sediment transport process in river flow can be represented as a quasi-steady process. Therefore, the available bed-load transport formulae and suspended load transport formulae can be applied for transport rate predictions.

Flume and field data show that the sand transport rate is most strongly related to the depth-averaged velocity. The power of velocity is approximately 3 to 4.
The bed material in natural conditions consists of non-uniform sediment particles. The effect of the non-uniformity of the sediments will result in selective transport processes (grain sorting). Grain sorting is related to the selective movement of sediment particles in a mixture near incipient motion at low bed-shear stresses and during generalized transport at higher shear stresses. Sorting effects can only be represented by taking the full size composition of the bed material, which may vary horizontally and vertically, into account.

3.2 Initiation of motion

Currents
Particle movement will occur when the instantaneous fluid force on a particle is just larger than the instantaneous resisting force related to the submerged particle weight and the friction coefficient. The degree of exposure of a grain with respect to surrounding grains (hiding of smaller particles resting or moving between the larger particles) obviously is an important parameter determining the forces at initiation of motion. Cohesive forces are important when the bed consists of appreciable amounts of clay and silt particles.
The driving forces are strongly related to the local near-bed velocities. In turbulent flow conditions the velocities are fluctuating in space and time. This makes together with the randomness of both particle size, shape and position that initiation of motion is not merely a deterministic phenomenon but a stochastic process as well.
The fluid forces acting on a sediment particle resting on a horizontal bed consist of skin friction forces and pressure forces. The skin friction force acts on the surface of the particles by viscous shear. The pressure force consisting of a drag and a lift force is generated by pressure differences along the surface of the particle. These forces per unit bed surface area can be reformulated in a time-averaged bed-shear stress.

Initiation of motion in steady flow is defined to occur when the dimensionless bed-shear stress (θ) is larger than a threshold value (θ_{cr}).

Thus, $\theta > \theta_{cr}$,

with:
$\tau_{b,c}/[(\rho_s-\rho_w)gd_{50}]$= particle mobility number,
$\tau_{b,c}$ = current-related bed-shear stress,
ρ_s = sediment density,
ρ_w = fluid density,
d_{50} = median sediment diameter.

The θ_{cr}-factor depends on the hydraulic conditions near the bed, the particle shape and the particle position relative to the other particles. The hydraulic conditions near the bed can be expressed by the Reynolds number $Re_* = u_*d/\nu$.

Thus: $\theta_{cr} = F(Re_*)$.

Many experiments have been performed to detemine the θ_{cr}-values as a function of Re_*. The experimental results of **Shields (1936)** related to a flat bed surface are most widely used to represent the critical conditions for initiation of motion (see Figure 1). The curve represents a critical stage at which only a minor part (say 1% to 10%) of the bed surface is moving.

Initiation of motion in combined steady and oscillatory flow (wave motion) can also be expressed in terms of the Shields parameters (**Van Rijn, 1993**).

Initiation of motion can also be expressed as function of a dimensionless particle size D_*.
The D_* parameter is defined as:

$$D_*= [\{u_*d/\nu\} \{1/\theta^{0.5}\}]^{2/3} = [\{u_*d/\nu\} \{((s-1)g\ d)^{0.5}/u_*\}]^{2/3} = [\{(s-1)^{0.5}\,g^{0.5}\,d^{1.5}/\nu\}]^{2/3} = (s-1)^{1/3}\,g^{1/3}\,d/\nu^{2/3}= d\ [(s-1)g/\nu^2]^{1/3}$$

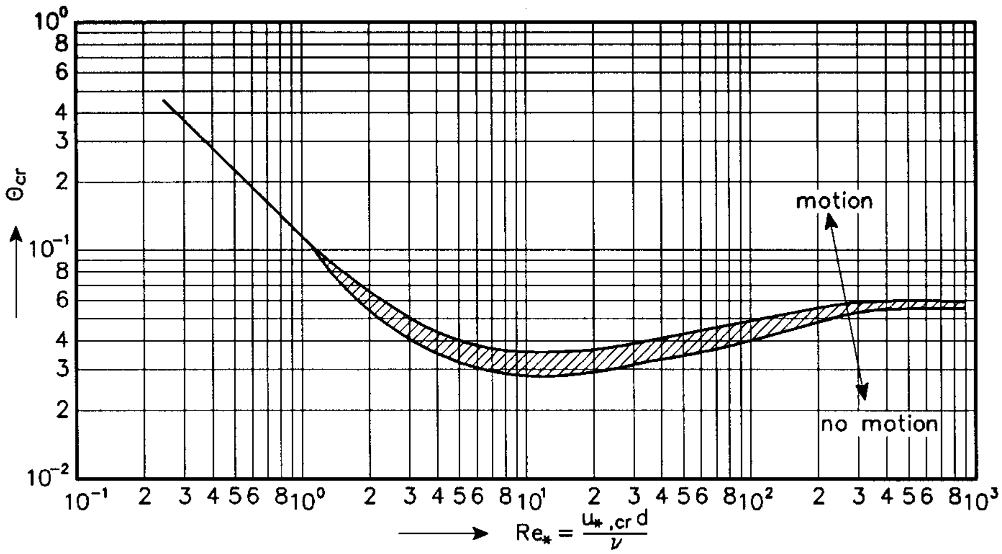

Figure 1 *Initiation of motion according to Shields (1936) as function of Reynolds number*

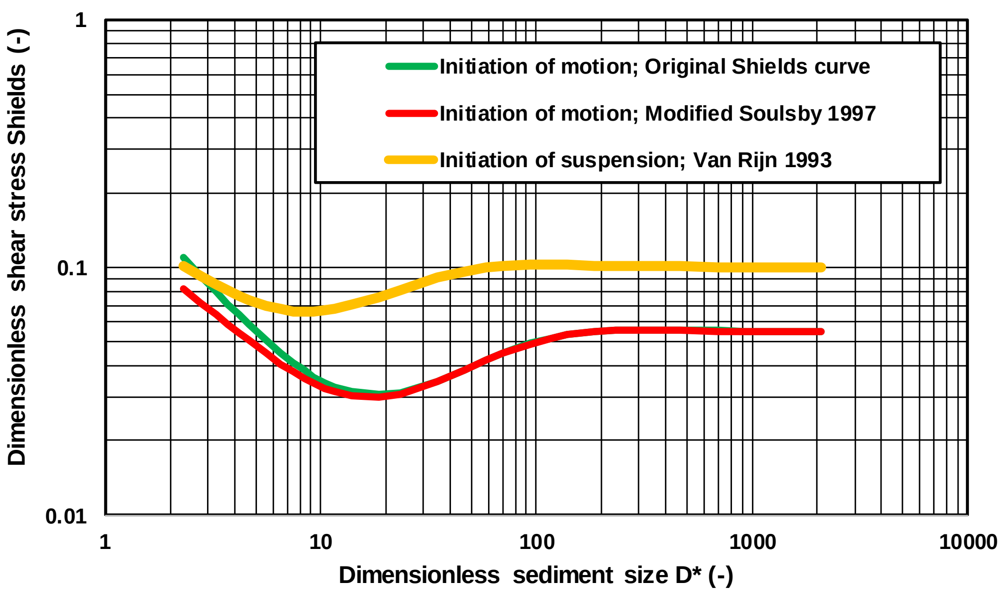

Figure 2 *Initiation of motion and suspension as function of dimensionless sediment size D_**

A simple expression for initiation of motion (movement of particles along the bed) is given by (Soulsby, 1997):

$$\theta_{cr,motion} = 0.3/(1+1.2\ D_*) + 0.055\ [1-\exp(-0.02D_*)] \quad (3.1)$$

with:

D_* = d_{50} $[(s-1)\ g/\nu^2]^{1/3}$ = dimensionless sediment size (m),
θ = $\tau_{b,c}/[(\rho_s-\rho_w)gd_{50}]$ = Shields parameter (-),
d_{50} = sediment particle size (m),
g = acceleration of gravity (m/s^2),
ν = kinematic viscosity coefficient (m^2/s),
s = ρ_s/ρ_w= relative density (-),
ρ_s = sediment density (kg/m^3),
ρ_w = water density (kg/m^3),

A simple expression for initiation of suspension (particles moving in suspension) is given by:

$$\theta_{cr,suspension} = 0.3/(1+ D_*) + 0.1\ [1-\exp(-0.05D_*)] \quad (3.2)$$

Equations (3.1) and (3.2) are shown in **Figure 2**.

Both equations can be used to compute the critical depth-averaged velocity for initiation of motion and suspension, as follows:

$$U_{critical,\ motion} = 5.75\ [\log(12h/(6D_{50}))]\ [\theta_{cr,motion}\ (s-1)\ g\ D_{50}]^{0.5} \quad (3.3)$$

$$U_{critical,\ suspension} = 5.75\ [\log(12h/(6D_{50}))]\ [\theta_{cr,suspension}\ (s-1)\ g\ D_{50}]^{0.5} \quad (3.4)$$

with:

θ = $\tau_{b,c}/[(\rho_s-\rho_w)gD_{50}]$ = Shields parameter (-),
$\tau_{b,c}$ = $\rho_w\ g\ U^2/C^2$ = bed-shear stress (N/m^2),
u_* = bed-shear velocity (m/s),
U = depth-averaged velocity (m/s),
C = $5.75\ g^{0.5}\ \log\{12h/(\alpha d_{90})\}$ = Chézy coefficient for rough flow conditions ($m^{0.5}/s$),
C = $5.75\ g^{0.5}\ \log\{12h/(\alpha d_{90}+3.3\nu/u_*)\}$= $5.75\ g^{0.5}\ \log\{12h/(\alpha d_{90}+ 1.05\ \nu C/U)\}$=
= Chézy coefficient for smooth turbulent flow conditions ($m^{0.5}/s$),
α = coeficient= 1 to 3 (α=1 for coarse grains; α=3 for fine grains),
ν = kinematic viscosity coefficient ($\cong 10^{-6}\ m^2/s$ for clear water),
h = water depth (m),
s = ρ_s/ρ_w = relative density (-),
d_{90} = $2d_{50}$ = 90% particle size (m).

Simple approximation formulae (10% accurate) are:

$U_{cr,motion} = 0.19(d_{50})^{0.1}\log(12h/6d_{50})$ for $0.0001<d_{50}<0.0005$ m; (3.5)
$U_{cr,motion} = 8.5(d_{50})^{0.6}\log(12h/6d_{50})$ for $0.0005<d_{50}<0.002$ m;
$U_{critical,\ suspension} = 2.8\ [h/d_{50}]^{0.1}\ [(s-1)\ g\ d_{50}]^{0.5}$ for $0.0001<d_{50}<0.002$ m; (3.6)

Figure 3 shows the critical depth-averaged velocities at initiation of motion and suspension for sediment with d_{50} between 0.1 and 2 mm based on Equations (3.3) and (3.4).

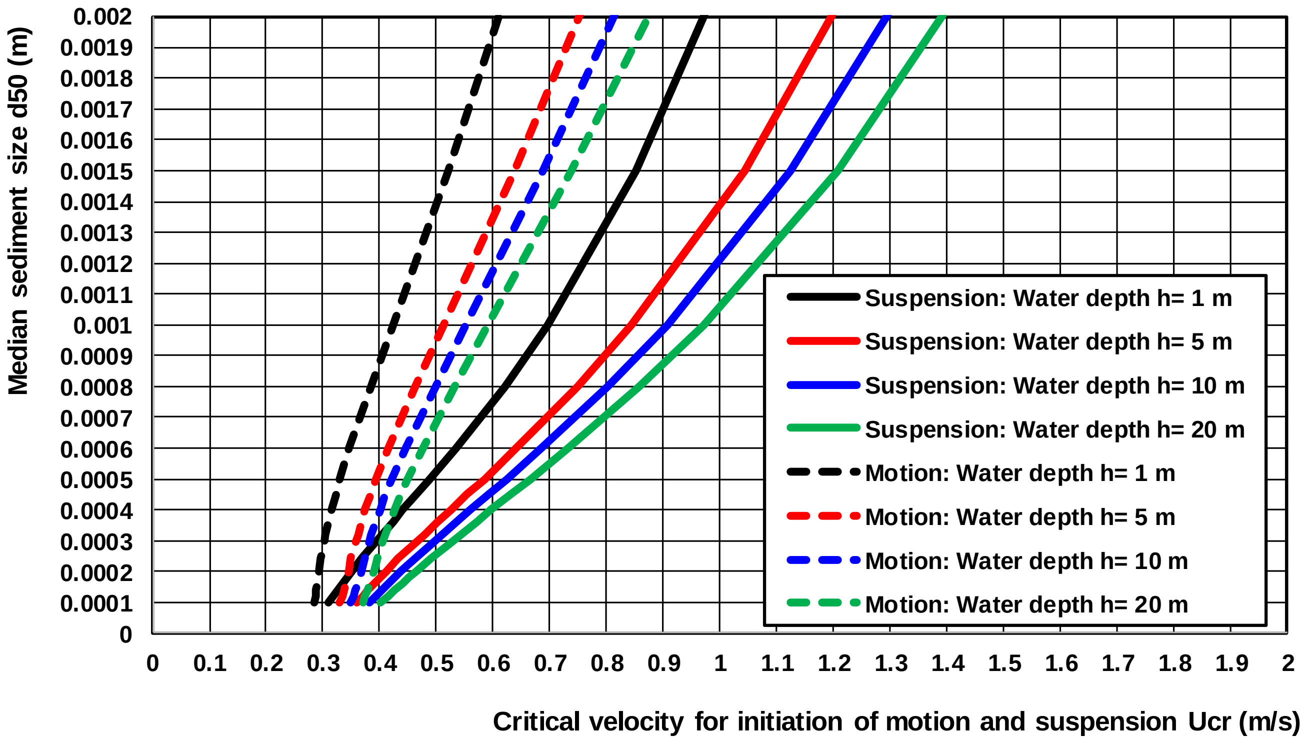

Figure 3 *Depth-averaged velocity at initiation of motion and suspension*

<u>Waves</u>

The Shields-curve can also be used for oscillatory flow as present under surface waves. The bed-shear stress is defined as (Van Rijn 1993, 2012):

$$\tau_{b,w} = \rho_w \, (u_{*,w})^2 = 0.25 \, \rho \, f_w \, (u_w)^2 \tag{3.7}$$

$$f_w = \exp(-6+5.2(A_w/k_{s,w})^{-0.19}) \quad \text{for rough oscillatory flow} \tag{3.8}$$

$$f_w = 0.09(U_w A_w/\nu)^{-0.2} \quad \text{for smooth oscillatory flow} \tag{3.9}$$

$$f_w = 2(U_w A_w/\nu)^{-0.5} \quad \text{for laminar oscillatory flow} \tag{3.10}$$

with:

$\tau_{b,w}$ = wave-related bed-shear stress;

U_w= peak orbital velocity= π $H_s/\{T_p \sinh(kh)\}$, (linear wave theory);

H_s= significant wave height;

L= wave length;

A_w= $T_p/(2\pi)U_w$ =peak orbital excursion;

T_p= peak wave period;

k=2π/L= wave number;

f_w= wave-related friction coefficient;

$k_{s,w}$= wave-related bed roughness.

Table 1 shows computed wave friction factors for low, medium and high waves and sand of 0.1, 0.5 and 1 mm. The friction factor values for smooth flow conditions are most valid for fine sediments < 0.3 mm.

Using: $\tau_{b,critical,shields} = 0.25\ \rho\ f_w\ (U_{w,cr})^2$, initiation of motion due to oscillatory flow with low waves over a plane bed:
d_{50}= 0.1 mm; D_*=2.5; $\tau_{b,critical,shields}$ = 0.15 N/m^2; f_w= 0.008 yields: $U_{w,cr}$= $[0.15/(0.25x1025x0.008)]^{0.5}$= 0.27 m/s,
d_{50}= 0.5 mm; D_*=12.5; $\tau_{b,critical,shields}$ = 0.25 N/m^2; f_w= 0.010 yields: $U_{w,cr}$= $[0.25/(0.25x1025x0.010)]^{0.5}$= 0.3 m/s,
d_{50}= 1 mm; D_*=25; $\tau_{b,critical,shields}$ = 0.50 N/m^2; f_w= 0.012 yields: $U_{w,cr}$= $[0.50/(0.25x1025x0.012)]^{0.5}$= 0.40 m/s.

Type of waves	**U_w (m/s)**	**A_w (m)**	**ν (m^2/s)**	**Friction factor f_w (-)**		
				d_{50}=0.1 mm	**d_{50}=0.5 mm**	**d_{50}=1 mm**
Low	0.5	0.5	10^{-6}	RT: 0.007-0.012 (k_s=0.1-1 mm) ST: 0.0075 L: 0.004	0.01-0.014 (k_s=0.5-1.5 mm) 0.0075 0.004	0.012-0.018 (k_s=1-3 mm) 0.0075 0.004
Medium	1	1	10^{-5}	RT: 0.008-0.014 (k_s=0.5-3 mm) ST: 0.009 L: 0.007	0.008-0.014 (k_s=1-3 mm) 0.009 0.007	0.014-0.017 (k_s=3-5 mm) 0.009 0.007
High	1.5	1.5	10^{-4}	RT: 0.009-0.018 (k_s=1-10 mm) ST: 0.012 L: 0.013	0.012-0.018 (k_s=3-10 mm) 0.012 0.013	0.014-0.018 (k_s=5-10mm) 0.012 0.013

1) Kinematic viscosity coefficient increases due to presence of sand
2) RT=rough turbulent; ST=smooth turbulent; L= laminar

Table 1 *Wave-related friction factors for plane bed with oscillatory flow*

3.3 Bed forms

Bed forms are relief features initiated by the fluid motions generated downstream of small local obstacles at the bottom consisting of movable (alluvial) sediment materials. Many types of bed forms can be observed in nature. The bed form regimes for steady flow over a sand bed can be classified into (see **Figure 4**):

- lower transport regime with flat bed, ribbons and ridges, ripples, dunes and bars,
- transitional regime with washed-out dunes and sand waves,
- upper transport regime with flat mobile bed and sand waves (anti-dunes).

When the bed form crest is perpendicular (transverse) to the main flow direction, the bed forms are called transverse bed forms, such as ripples, dunes and anti-dunes.
Ripples have a length scale much smaller than the water depth, whereas dunes have a length scale much larger than the water depth. The crest lines of the bed forms may be straight, sinuous, linguoid or lunate. Ripples and dunes travel downstream by erosion at the upstream face (stoss-side) and deposition at the downstream face (lee-side). Antidunes travel upstream by lee-side erosion and stoss-side deposition. Bed forms with their crest parallel to the flow are called longitudinal bed forms such as ribbons and ridges.

In the literature, various bed-form classification methods for sand beds are presented. The types of bed forms are described in terms of basic parameters (Froude number, suspension parameter, particle mobility parameter; dimensionless particle diameter).

A flat immobile bed may be observed just before the onset of particle motion, while a flat mobile bed will be present just beyond the onset of motion. The bed surface before the onset of motion may also be covered with relict bed forms generated during stages with larger velocities.

Small-scale ribbon and ridge type bed forms parallel to the main flow direction have been observed in laboratory flumes and small natural channels, especially in case of fine sediments (d_{50} < 0.1 mm) and are probably generated by secondary flow phenomena and near-bed turbulence effects (burst-sweep cycle) in the lower and transitional flow regime. These bed forms are also known as parting lineations because of the streamwise ridges and hollows with a vertical scale equal to about 10 grain diameters and these bed forms are mostly found in fine sediments (say 0.05 to 0.25 mm).

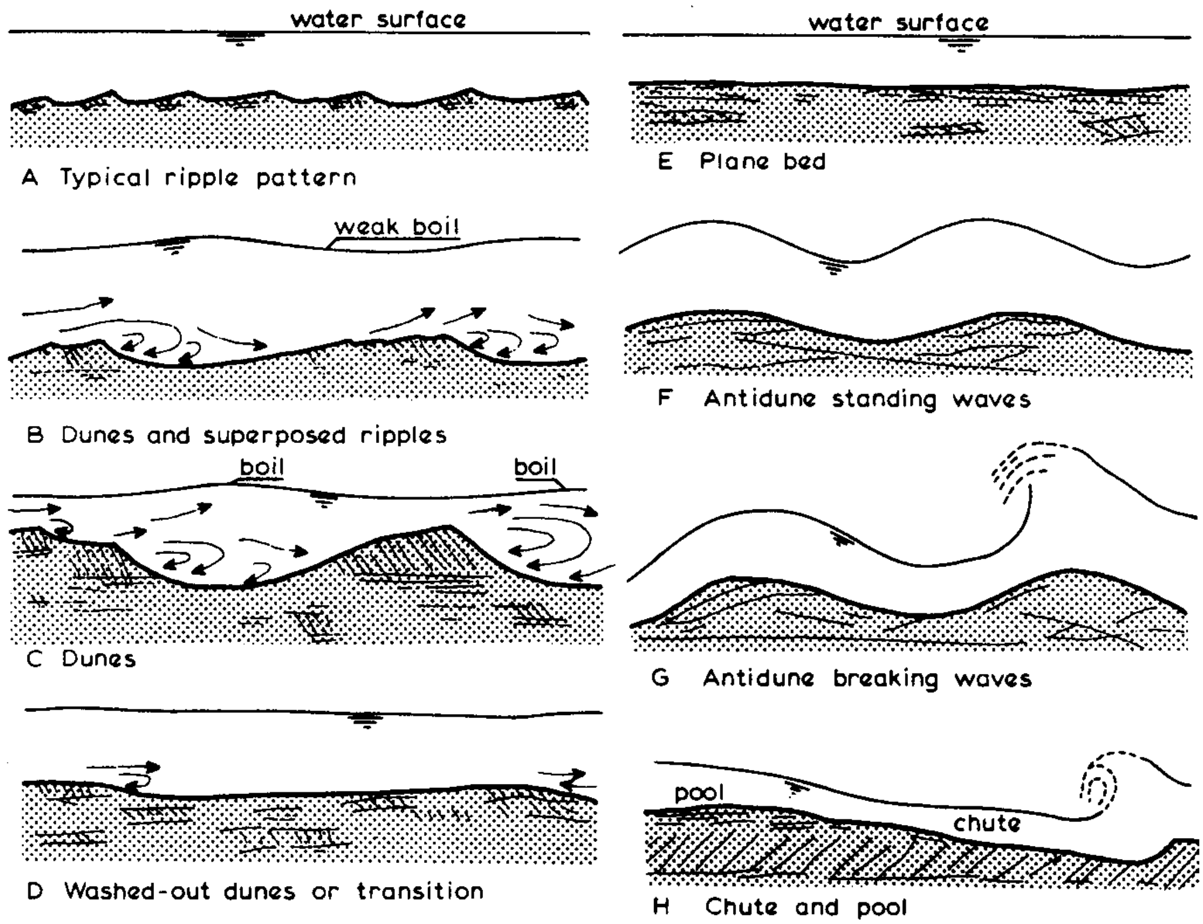

Figure 4 *Bed forms in steady flows (rivers)*

When the velocities are somewhat larger (10%-20%) than the critical velocity for initiation of motion and the median particle size is smaller than about 0.5 mm, small (mini) ripples are generated at the bed surface. Ripples that are developed during this stage remain small with a ripple length much smaller than the water depth.
The characteristics of mini ripples are commonly assumed to be related to the turbulence characteristics near the bed (burst-sweep cycle). Current ripples have an asymmetric profile with a relatively steep downstream face (lee-side) and a relatively gentle upstream face (stoss-side). As the velocities near the bed become larger, the ripples become more irregular in shape, height and spacing yielding strongly three-dimensional ripples. In that case the variance of the ripple length and height becomes rather large. These ripples are known as lunate ripples when the ripple front has a concave shape in the current direction (crest is moving slower than wing tips) and are called linguoid ripples when the ripple front has a convex shape (crest is moving faster than wing tips). The largest ripples may have a length up to the water depth and are commonly called mega-ripples.

Another typical bed form type of the lower regime is the dune-type bed form. Dunes have an asymmetrical (triangular) profile with a rather steep lee-side and a gentle stoss-side. A general feature of dune type bed forms is lee-side flow separation resulting in strong eddy motions downstream of the dune crest. The length of the dunes is

strongly related to the water depth (h) with values in the range of 3 to 15 h. Extremely large dunes with heights (Δ) of the order of 7 m and lengths (λ) of the order of 500 m have been observed in the Rio Parana River (Argentina) at water depths of about 25 m, velocities of about 2 m/s and bed material sizes of about 0.3 mm.
The formation of dunes may be caused by large-scale fluid velocity oscillations generating regions at regular intervals with decreased and increased bed-shear stresses, resulting in the local deposition and erosion of sediment particles.

The largest bed forms in the lower regime are sand bars (such as alternate bars, side bars, point bars, braid bars and transverse bars), which usually are generated in areas with relatively large transverse flow components (bends, confluences, expansions). Alternate bars are features with their crests near alternate banks of the river. Braid bars actually are alluvial "islands" which separate the anabranches of braided streams. Numerous bars can be observed distributed over the cross-sections. These bars have a marked streamwise elongation. Transverse bars are diagonal shoals of triangular-shaped plan along the bed. One side may be attached to the channel bank. These type of bars generally are generated in steep slope channels with a large width-depth ratio. The flow over transverse bars is sinuous (wavy) in plan. Side bars are bars connected to river banks in a meandering channel. There is no flow over the bar. The planform is roughly triangular. Special examples of side bars are point bars and scroll bars.

It is a well-known phenomenon that the bed forms generated at low velocities are washed out at high velocities. It is not clear, however, whether the disappearance of the bed forms is accomplished by a decrease of the bed form height, by an increase of the bed form length or both. Flume experiments with sediment material of about 0.45 mm show that the transition from the lower to the upper regime is effectuated by an increase of the bed form length and a simultaneous decrease of the bed form height. Ultimately, relatively long and smooth sand waves with a roughness equal to the grain roughness were generated (**Van Rijn, 1993**).

In the transition regime the sediment particles will be transported mainly in suspension. This will have a strong effect on the bed form shape. The bed forms will become more symmetrical with relatively gentle lee-side slopes. Flow separation will occur less frequently and the effective bed roughness will approach to that of a plane bed. Large-scale bed forms with a relative height (Δ/h) of 0.1 to 0.2 and a relative length (λ/h) of 5 to 15 were present in the Mississippi river at high velocities in the upper regime.

In the supercritical upper regime the bed form types will be plane bed and/or anti-dunes. The latter type of bed forms are sand waves with a nearly symmetrical shape in phase with the water surface waves. The anti-dunes do not exist as a continuous train of bed waves, but they gradually build up locally from a flat bed. Anti-dunes move upstream due to strong lee-side erosion and stoss-side deposition. Anti-dunes are bed forms with a length scale of about 10 times the water depth ($\lambda \cong 10$ h). When the flow velocity further increases, finally a stage with chute and pools may be generated.

3.4 Bed roughness

Nikuradse (1932) introduced the concept of an equivalent or effective sand roughness height (k_s) to simulate the roughness of arbitrary roughness elements of the bottom boundary. In case of a movable bed consisting of sediments the effective bed roughness (k_s) mainly consists of grain roughness ($k^{/}_{s}$) generated by skin friction forces and of form roughness ($k^{//}_{s}$) generated by pressure forces acting on the bed forms. Similarly, a grain-related bed-shear stress ($\tau^{/}_{b}$) and a form-related bed-shear stress ($\tau^{//}_{b}$) can be defined. The effective bed roughness for a given bed material size is not constant but depends on the flow conditions. Analysis results of k_s-values computed from Mississippi River data (USA) show that the k_s-value strongly decreases from about 0.5 m at low velocities (0.5 m/s) to about 0.001 m at high velocities (2 m/s), probably because the bed forms become more rounded or are washed out at high velocities.

The effective bed-shear stresses related to the movement of sediment particles can be represented as:

$$\tau_{b,c}' = \mu_c \ \tau_{b,c} \qquad (3.11)$$
$$\tau_{b,w}' = \mu_w \ \tau_{b,w} \qquad (3.12)$$

μ_c= current-related efficiency factor (0.1-0.2),
μ_w= wave-related efficiency factor (0.1-0.3).

The fundamental problem of bed roughness prediction is that the bed characteristics (bed forms) and hence the bed roughness depend on the main flow variables (depth, velocity) and sediment transport rate (sediment size). These hydraulic variables are, however, in turn strongly dependent on the bed configuration and its roughness.
Another problem is the almost continuous variation of the discharge during rising and falling stages. Under these conditions the bed form dimensions and hence the Chézy-coefficient are not constant but vary with the flow conditions.

3.5 Bed load transport

The transport of particles by rolling, sliding and saltating is known as the bed-load transport. For example, **Bagnold (1956)** defines the bed-load transport as that in which the successive contacts of the particles with the bed are strictly limited by the effect of gravity, while the suspended-load transport is defined as that in which the excess weight of the particles is supported by random successions of upward impulses imported by turbulent eddies. **Einstein (1950)**, however, has a somewhat different approach. Einstein defines the bed-load transport as the transport of sediment particles in a thin layer of 2 particle diameters thick just above the bed by sliding, rolling and sometimes by making jumps with a longitudinal distance of a few particle diameters. The bed layer is considered as a layer in which the mixing due to the turbulence is so small that it cannot influence the sediment particles, and therefore suspension of particles is impossible in the bed-load layer. Further, Einstein assumes that the average distance travelled by any bed-load particle (as a series of successive movements) is a constant distance of 100 particle diameters, independent of the flow condition, the transport rate and the bed composition. In the view of Einstein, the saltating particles belong to the suspension mode of transport, because the jump lengths of saltating particles are considerably larger than a few grain diameters.

The first reliable empirical bed load transport formula was presented by **Meyer-Peter and Mueller (1948)**. They performed flume experiments with uniform particles and with particle mixtures. Based on data analysis, a relatively simple formula was obtained, which is frequently used.
Einstein (1950) introduced statistical methods to represent the turbulent behaviour of the flow. Einstein gave a detailed but complicated statistical description of the particle motion in which the exchange probability of a particle is related to the hydrodynamic lift force and particle weight. Einstein proposed the d_{35} as the effective diameter for particle mixtures and the d_{65} as the effective diameter for grain roughness.
Bagnold (1966) introduced an energy concept and related the sediment transport rate to the work done by the fluid.
Engelund and Hansen (1967) presented a simple and reliable formula for the total load transport in rivers.
Van Rijn (1984) solved the equations of motions of an individual bed-load particle and computed the saltation characteristics and the particle velocity as a function of the flow conditions and the particle diameter for plane bed conditions.
The results of sensitivity computations show that the bed load transport is only weakly affected by particle diameter. A 25%-variation of the particle diameter (d_m = 0.8±0.2 mm) results in a 10%-variation of the transport rate.

Bed load transport (q_b) can be determined from the measured bed form dimensions and the measured bed form migration velocity using echo sounding results. The bed load transport is by definition: mass m_s per unit area of bed m_s (kg/m^2) times migration velocity c (m/s).
Thus: $q_b = m_s\, c$ (in kg/m/s).

The mass (M_s) of a triangular bed form with length L, height ΔH, sediment density ρ_s ($\cong$2650 kg/m^3) and porosity p ($\cong$0.4) is $M_s = \rho_s (1-p)\ 0.5\ \Delta H\ L$.
The mass per unit area is the mass M_s divided by the length L giving: $m_s = \rho_s (1-p)\ 0.5\ \Delta H$.
The migration velocity is c.
Bed load transport is: $q_b = 0.5\ \rho_s (1-p)\ \Delta H\ c$.
As bed forms are not fully triangular, a more general expression is: $q_b = \alpha\ \rho_s (1-p)\ \Delta H\ c$ with α = 0.5 to 0.7.

3.6 Suspended load transport

When the value of the bed-shear velocity exceeds the particle fall velocity, the particles can be lifted to a level at which the upward turbulent forces will be comparable to or higher than the submerged particle weight resulting in random particle trajectories due to turbulent velocity fluctuations. The particle velocity in longitudinal direction is almost equal to the fluid velocity. Usually, the behaviour of the suspended sediment particles is described in terms of the sediment concentration, which is the solid volume (m^3) per unit fluid volume (m^3) or the solid mass (kg) per unit fluid volume (m^3).

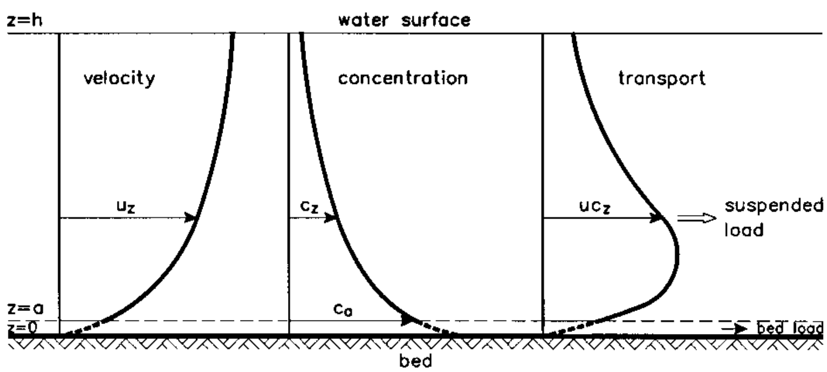

Figure 5 *Definition sketch of suspended sediment transport*

Observations show that the suspended sediment concentrations decrease with distance up from the bed. The rate of decrease depends on the ratio of the fall velocity and the bed-shear velocity (w_s/u_*).
The depth-integrated suspended-load transport ($q_{s,c}$) is herein defined as the integration of the product of velocity (u) and concentration (c) from the edge of the bed-load layer (z=a) to the water surface (z=h).

This definition requires the determination of the velocity profile, concentration profile and a known concentration (c_a) close to the bed (z=a), see **Figure 5**. These latter parameters are refered to as the *reference concentration* and the *reference level*: c_a at z=a.

Sometimes, the suspended load transport is given as a mean volumetric concentration defined as the ratio of the volumetric suspended load transport (= sediment discharge) and the flow discharge: $c_{mean}=q_{s,c}/q$.

The mean concentration (c_{mean}) is approximately equal to the depth-averaged concentration for fine sediments (mud).

The concentration can be expressed as a weight concentration (c_g) in kg/m^3 or as a volume concentration (c_v) in m^3/m^3.
Sometimes the volume concentration is expressed as a volume percentage after multiplying with 100%.

Some rivers carry very high concentrations of fine sediments (particles < 0.05 mm), usually refered to as the wash load. Experience shows that the presence of fines enhances the suspended sand transport rate because the fluid viscosity and density are increased by the fine sediments. As a result the fall velocity of the suspended sand particles will be reduced with respect to that in clear water and hence the suspended sand transport capacity of the flow will increase.

The sediment concentration distribution over the water depth can be described by the diffusion approach, which yields for steady, uniform flow (**Van Rijn, 1993, 2012**):

$$c\, w_s + \varepsilon_s\, dc/dz = 0 \qquad (3.13)$$

with
c = sand concentration,
w_s = particle fall velocity and
ε_s = sediment diffusivity coefficient.

Using a parabolic sediment diffusivity coefficient over the depth, the concentration profile can be expressed by the **Rouse** profile:

$$c/c_a = [((h-z)/z)\, (a/(h-a))]^{ws/\kappa u^*} \qquad (3.14)$$

with:
h = water depth,
a = reference level,
z = height above bed,
c_a = reference concentration,
w_s = particle fall velocity,
u_* = bed-shear velocity,
κ = Von Karmann coefficient (=0.4).

The relative importance of the suspended load transport is determined by the suspension number $Z=w_s/\kappa u_*$.

The following values can be used:

$Z=5$: suspended sediment in near-bed layer ($z<0.1h$),

$Z=2$: suspended sediment up to mid of water depth ($z<0.5h$),

$Z=1$: suspended sediment up to water surface ($z<h$),

$Z=0.1$: suspended sediment almost uniformly distributed over water depth.

4. Sand transport in non-steady (tidal) flow

In non-steady flow the actual sediment transport rate may be smaller (underload) or larger (overload) than the transport capacity resulting in net erosion or deposition assuming sufficient availability of bed material (no armour layers).
Bed-load transport in non-steady flow can be modelled by a formula type of approach because the adjustment of the transport of sediment particles close to the bed proceeds rapidly to the new hydraulic conditions.
Suspended load transport, however, does not have such a behaviour because it takes time (time lag effects) to transport the particles upwards and downwards over the depth and therefore it is necessary to model the vertical convection-diffusion process.

4.1 Effect of time lag

Tidal flow is characterized by a daily ebb and flood cycle with a time scale of 6 to 12 hours (semidiurnal or diurnal tide) and by a neap-spring cycle with a time scale of about 14 days.
Sediment concentration measurements in tidal flow over a fine sand bed (0.05 to 0.3 mm) show a continuous adjustment of the concentrations to the flow velocities with a lag period in the range of 0 to 60 minutes

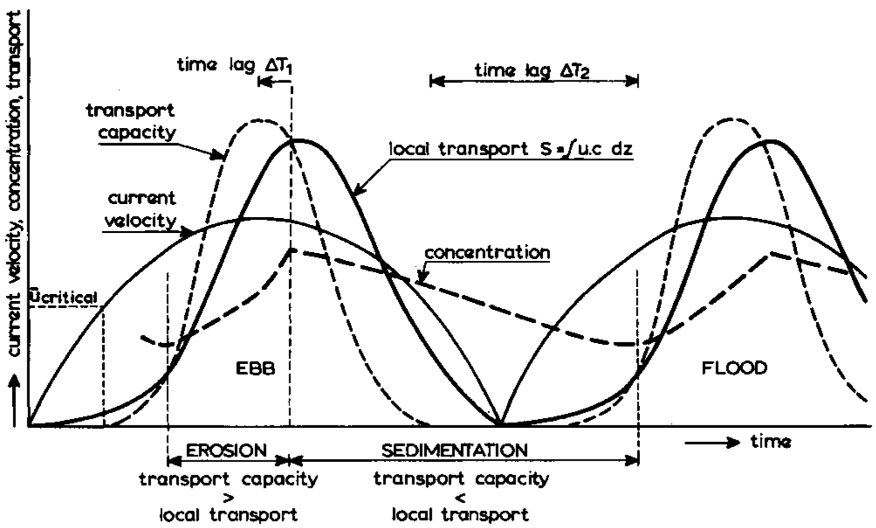

Figure 6 *Time lag of suspended sediment concentrations in tidal flow*

The basic transport process in tidal flow is shown in **Figure 6**. Sediment particles go into suspension when the current velocity exceeds a critical value. In accelerating flow there always is a net vertical upward transport of sediment particles due to turbulence-related diffusive processes, which continues as long as the sediment transport capacity exceeds the actual transport rate. The time lag period ΔT_1 is the time period between the time of maximum flow and the time at which the transport capacity is equal to the actual transport rate. After this latter time there is a net downward sediment transport because settling dominates yielding smaller concentrations and transport rates. In case of very fine sediments (silt) or a large depth, the settling process can continue during the slack water period giving a large time lag (ΔT_2) which is defined as the period between the time of zero transport capacity and the start of a new erosion cycle. **Figure 6** shows that the suspended sediment transport during decelerating flow is always larger than during accelerating flow.

Time lag effects can be neglected for sediments larger than about 0.3 mm and hence a quasi-steady approach based on the available sediment transport formulae can be applied.

4.2 Effect of salinity stratification

In a stratified estuary a high-density salt wedge exists in the near-bed region resulting in relatively high near-bed densities and relatively low near-surface densities. Stratified flow will result in damping of turbulence because turbulence energy is consumed in the mixing of heavier fluid from a lower level to a higher level against the action of gravity.

The usual method to account for the salinity-related stratification effect on the velocity and concentration profiles is the reduction of the fluid mixing coefficient by introducing a damping factor related to the Richardson-number (Ri), as follows: $\varepsilon_f = \phi\ \varepsilon_{f,o}$ with $\varepsilon_{f,o}$=fluid mixing coefficient in fresh water, ϕ= F(Ri) = damping factor (< 1), Ri= local Richardson number.

The ϕ-factor can be represented by a function given by **Munk-Anderson (1948)**: $\phi = (1 + 3.3\ Ri)^{-1.5}$.

The simple sand transport formulae do not give realistic results when the salinity-related damping effect is significant (vertical density gradient in stratified flow).

4.3 Effect of mud

In most tidal basins the sediment bed consists of a mixture of sand and mud. The sand-mud mixture generally behaves as a mixture with cohesive properties when the mud fraction (all sediments < 0.05 mm) is dominant (> 0.3) and as a non-cohesive mixture when the sand fraction is dominant (> 0.7). The distinction between non-cohesive mixtures and cohesive mixtures can be related to a critical mud content ($p_{mud,cr}$). Most important is the value of the clay-fraction (sediments < 0.005 mm) in the mixture. Cohesive properties become dominant when the clay-fraction is larger than about 5% to 10%. Assuming a clay-mud ratio of 1/2 to 1/4 for natural mud beds, the critical mud content will be about $p_{mud,cr}$= 0.2 to 0.4.

If the mud content is below the critical value ($p_{mud}<p_{mud,cr}$), the sand-mud mixture can be assumed to be homogeneous with depth and to have non-cohesive properties. Furthermore, the erosion of the sand particles is the dominant erosion mechanism. The mud particles will be washed out together with the sand particles. Laboratory and field observations (**Van Rijn, 1993**) have shown that the erosion or pick-up process of the sand particles is slowed down by the presence of the mud particles. This behaviour can be quite well modelled by increasing the critical bed-shear stress for initiation of motion of the sand particles. Herein, it is assumed that: $\tau_{b,cr,sand}=(1+p_{mud})^{\beta}\ \tau_{b,cr,shields}$ with β=3 based on analysis of field data.

5. Sand transport in non-steady coastal flows

Sand transport in a coastal environment generally occurs under the combined influence of a variety of hydrodynamic processes such as winds, waves and currents.

Sand can be transported by wind-, wave-, tide- and density-driven currents (current-related or advective transport), by the oscillatory water motion itself (wave-related or oscillating transport) as caused by the deformation of short waves under the influence of decreasing water depth (wave asymmetry), or by a combination of currents and short waves.

The waves generally act as sediment stirring agents; the sediments are transported by the mean current. Low-frequency waves interacting with short waves may also contribute to the sediment transport process. Wind-blown sand represents another basic transport process in the beach-dune zone.

In friction-dominated deeper water outside the breaker (surf) zone the transport process is generally concentrated in a layer close to the sea bed; bed-load transport (bed form migration) and suspended transport may be equally important. Bed load type transport dominates in areas where the mean currents are relatively weak in comparison with the wave motion (small ratio of depth-averaged velocity and peak orbital velocity). Suspension of sediments can be caused by ripple-related vortices. The suspended load transport becomes increasingly important with increasing strength of the tide- and wind-driven mean current, due to the turbulence-related mixing capacity of the mean current (shearing in boundary layer). By this mechanism the sediments are mixed up from the bed-load layer to the upper layers of the flow.

In the surf zone of sandy beaches the transport is generally dominated by waves through wave breaking and the associated wave-induced currents in the longshore and cross-shore directions. The longshore transport in the surf zone is also known as the longshore drift. The breaking process together with the near-bed wave-induced oscillatory water motion can bring relatively large quantities of sand into suspension (stirring) which is then transported as suspended load by net (wave-cycle averaged) currents such as tide-, wind- and density (salinity)-driven currents. The concentrations are generally maximum near the plunging point and decrease sharply on both sides of this location.

The nature of the sea bed (plane or rippled bed) has a fundamental role in the transport of sediments by waves and currents. The configuration of the sea bed controls the near-bed velocity profile, the shear stresses and the turbulence and, thereby, the mixing and transport of the sediment particles. For example, the presence of ripples reduces the near-bed velocities, but it enhances the bed-shear stresses, turbulence and the entrainment of sediment particles resulting in larger overall suspension levels. Several types of bed forms can be identified, depending on the type of wave-current motion and the bed material composition. Focussing on fine sand in the range of 0.1 to 0.3 mm, there is a sequence starting with the generation of rolling grain ripples, to vortex ripples and, finally, to upper plane bed with sheet flow for increasing bed-shear. Rolling grain ripples are low relief ripples that are formed just beyond the stage of initiation of motion. These ripples are transformed into more pronounced vortex ripples due to the generation of sediment-laden vortices formed in the lee of the ripple crests under increasing wave motion. The vortex ripples are washed out under large storm waves (in shallow water) resulting in plane bed sheet flow characterised by a thin layer of large sediment concentrations.

6. Simple general formulae for sand transport in rivers, estuaries and coastal waters

6.1 Bed load transport

Van Rijn (1984, 1993) proposed a simplified formula for bed-load transport in current only conditions, which reads as:

$$q_b = \alpha_b \rho_s U h (d_{50}/h)^{1.2} (M_e)^{\eta} \qquad (6.1)$$

with:

$q_{b,c}$ = depth-integrated bed-load transport (kg/s/m),
M_e = $(U-U_{cr})/[(s-1)gd_{50}]^{0.5}$ (-),
U = depth-averaged velocity (m/s),
U_{cr} = critical depth-averaged velocity for initiation of motion (m/s),
d_{50} = median particle size (m),
h = water depth (m),
α_b = coefficient (-),
η = exponent (-),
ρ_s = sediment density (kg/m^3),
S = ρ_s/ρ_w = specific density (-).

The original α_b and n coefficients were found to be α=0.005 and η=2.4.
These values yield however bed-load transport rates, which are systematically too large for velocities >1 m/s and too small for velocities <1 m/s.

Therefore, both coefficients were recalibrated using measured bed load transport data (**Van Rijn 2007**), yielding α_b= 0.015 and η= 1.5.

All computed values are within a factor 2 from the measured bed load transport rates for velocities larger than 0.6 m/s. The measured values are underpredicted (factor 2 to 3) for velocities close to initiation of motion.
Equation (6.1) can be easily extended to coastal flow (steady flow plus waves) by introducing an effective velocity u_e consisting of the steady current velocity (u) plus the peak orbital velocity (U_w), as follows: $u_e=u+\gamma U_w$.

The γ-value was determined by calibration using computed values of the detailed, numerical intra-wave TR2004 model (**Van Rijn 2007**), yielding γ=0.4.

The new simplified bed load-load transport formula for steady flow (with or without waves) reads, as :

$$q_b = \alpha_b \, \rho_s \, U \, h \, (d_{50}/h)^{1..2} \, M_e^{1.5} \qquad (6.2)$$

with:
q_b = bed load transport)kg/s/m),
α_b = 0.015,
M_e = $(U_e-U_{cr})/[(s-1)gd_{50}]^{0.5}$= mobility parameter (-);
U_e = $U + \gamma U_w$= effective velocity (m/s) with γ=0.4 for irregular waves (and 0.8 for regular waves);
U = depth-averaged flow velocity (m/s);
U_w = $\pi H_s/[T_p \sinh(kh)]$= peak orbital velocity (m/s) based on linear wave theory;
H_s = significant wave height (m); T_p= peak wave period (s);
U_{cr} = $\beta u_{cr,c} + (1-\beta)u_{cr,w}$ = critical velocity (m/s) with $\beta=u/(u+U_w)$;
$U_{cr,c}$ = critical velocity (m/s) for currents based on Shields (initiation of motion see Van Rijn, 1993);
$U_{cr,w}$ = critical velocity (m/s) for waves (see Van Rijn, 1993);
$U_{cr,c}$ = $0.19(d_{50})^{0.1}\log(12h/3d_{90})$ for $0.0001<d_{50}<0.0005$ m;
$U_{cr,c}$ = $8.5(d_{50})^{0.6}\log(12h/3d_{90})$ for $0.0005<d_{50}<0.002$ m;
$U_{cr,w}$ = $0.24[(s-1)g]^{0.66} \, d_{50}^{0.33} \, (T_p)^{0.33}$ for $0.0001<d_{50}<0.0005$ m;
$U_{cr,w}$ = $0.95[(s-1)g]^{0.57} \, d_{50}^{0.43} \, (T_p)^{0.14}$ for $0.0005<d_{50}<0.002$ m.

The inaccuracies are largest (underprediction) for relatively low u_e-velocities (<0.5 m/s) close to the critical velocities.

Equation (6.2) describes the net bed load transport in current-dominated conditions (longshore flows). It cannot be used to compute the net cross-shore bed-load transport in the inner surf and swash zone. For these complicated conditions the full intra-wave method should be used.

6.2 Suspended load transport

The simplified suspended load transport formula for steady flow proposed by **Van Rijn (1984)** was extended to coastal flow (waves) and reads, as (see also **Soulsby, 1997**):

$$q_s = \alpha_s \rho_s U d_{50} M_e^{2.4} (D_*)^{-0.6} \quad (6.3a)$$

with:
q_s = suspended load transport (kg/s/m);
h = water depth (m),
d_{50} = particle size (m),
D_* = $d_{50}[(s-1)g/\nu^2]^{1/3}$= dimensionless particle size (m),
α_s = 0.012 (coefficient),
s = ρ_s/ρ_w = relative density (-),
ν = kinematic viscosity (m^2/s),
M_e = $(U_e-U_{cr})/[(s-1)gd_{50}]^{0.5}$= mobility parameter (see Equation 6.2),
U_e = effective velocity (see Equation 6.2),
U_{cr} = critical depth-averaged velocity for initiation of motion (see Equation 6.2).

The original α_s coefficient is α_s = 0.012 (**Van Rijn 1984**).

The most realistic variation range is α_s =0.008 to 0.012.

The best value matching the results of the detailed TR2004 results is α_s = 0.008 (see **Figure 7**); yielding for the suspended load transport:

$$q_s = 0.008 \rho_s U d_{50} M_e^{2.4} (D_*)^{-0.6} \quad (6.3b)$$

Equation (6.3a,b) defines the current-related suspended transport (q_s) which is the transport of sediment by the mean current including the effect of wave stirring on the sediment load.
The suspended transport of very fine sediments (<0.1 mm) is somewhat underestimated by Equation (6.3a,b).

Equation (6.3a,b) is based on the assumption that suspended load transport occurs for $U > U_{cr,motion}$ with $U_{cr,motion}$ based on Equation (3.3).
It is more physical to assume that suspended load transport occurs for $U > U_{cr,suspension}$ with $U_{cr,suspension}$ based on Equation (3.4).

Using this later approach, the suspended load transport is given by a slightly modified expression:

$$q_s = 0.03 \rho_s U d_{50} M_e^{2} (D_*)^{-0.6} \quad (6.4)$$

q_s = suspended load transport (kg/s/m),
h = water depth (m),
d_{50} = particle size (m),
D_* = $d_{50}[(s-1)g/\nu^2]^{1/3}$= dimensionless particle size (m),
s = ρ_s/ρ_w = relative density (-),
ν = kinematic viscosity (m^2/s),
M_e = $(U_e-U_{cr,suspension})/[(s-1)gd_{50}]^{0.5}$= mobility parameter (-),

U_e = effective velocity (m/s) including effect of waves (see Equation 6.2),
$U_{cr,suspension}$ = critical depth-averaged velocity (m/s) for initiation of suspension (Equation 3.4).

Figure 7 shows Equations (6.3a), (6.3b) and (6.4) for a water depth of h= 5 m, d_{50}= 0.00025 m. Measured transport rates (**green** trendline) based on the dataset given by Van Rijn (2007) are also shown. Equation (6.4) yield similar results except for very small velocities< 0.5 m.

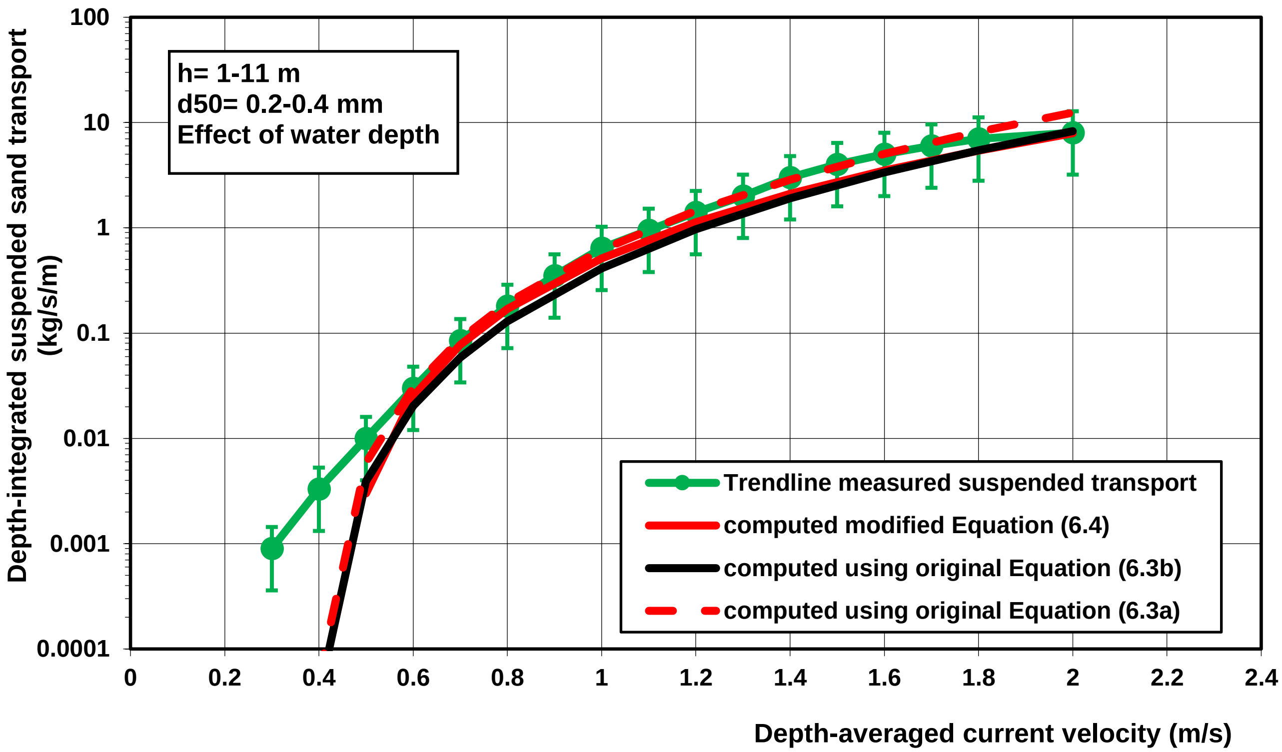

Figure 7 *Suspended transport as function of depth-averaged velocity*

6.3 Sand transport computations for combined wave plus current conditions in water depth of 5 m

The detailed TR2004 model (**Van Rijn 2007**) was used to compute the total sand transport rates (bed load plus suspended load transport) for a depth of 5 m and a median size of d_{50}= 250 μm (d_{10}= 125 μm, d_{90}= 500 μm).
The wave height was varied in the range of 0 to 3 m and wave periods in the range of 5 to 8 s.
The wave direction is assumed to be normal to the coast, whereas the current is assumed to be parallel to the coast (φ=90°). The temperature is 15 °C and the salinity is 0 (fluid density= 1000 kg/m^3).
The total load transport (bed load + suspended load) results of the TR2004 model are shown in **Figure 8** together with earlier results of the TR1993 model (**Van Rijn, 1993**) for the same parameter range. Some measured data of rivers and estuaries are also shown.
The total sand transport based on the simplified formulae (Equations (6.2) and (6.3a)) is also shown in **Figure 8**.
Table 2 shows some values based on Equation (6.2) with α_b =0.015 and Equation (6.3a,b), (6.4) for h= 5 m, v= 1 m/s and H_s= 0, 0.5, 1, 2 and 3 m/s.
It is noted that the transport rates are approximately equal for H_s= 0 and 0.5 m in the velocity range 1 to 2 m/s. Small waves of H_s=0.5 m in a depth of 5 m have almost no effect on the sediment transport rate for velocities larger than about 1 m/s, because the current-related mixing is dominant.
The **TR2004 model** yields slightly smaller values than the **TR1993 model** for the case without waves (H_s= 0 m).

The **TR2004 model** yields considerably smaller (up to factor 3) total load transport rates for a steady current with high waves (H_s=3 m) compared to the results of the **TR1993 model**. This is mainly caused by the inclusion of a damping factor acting on the wave-related near-bed diffusivity in the upper regime with storm waves.
The **TR2004** results for steady flow (without waves) show reasonable agreement with measured values (data from major rivers and estuaries with depth of about 5 m and sediment size of about 250 μm) over the full velocity range from 0.6 to 2 m/s.
The results of the **TR2004** show that the total transport varies with U^5 for H_s= 0 m; $U^{2.5}$ for H_s= 1 m and U^2 for H_s= 3 m.
The transport rate varies with H_s^3 for U= 0.5 m/s; with $H_s^{1.5}$ for U= 1 m/s and with H_s for U= 2 m/s.
The total transport rate (q_t=q_b+q_s) based on the simplified method generally are within a factor of 2 of the more detailed **TR2004 model**. The simplified method tend to underpredict for low and high velocities.

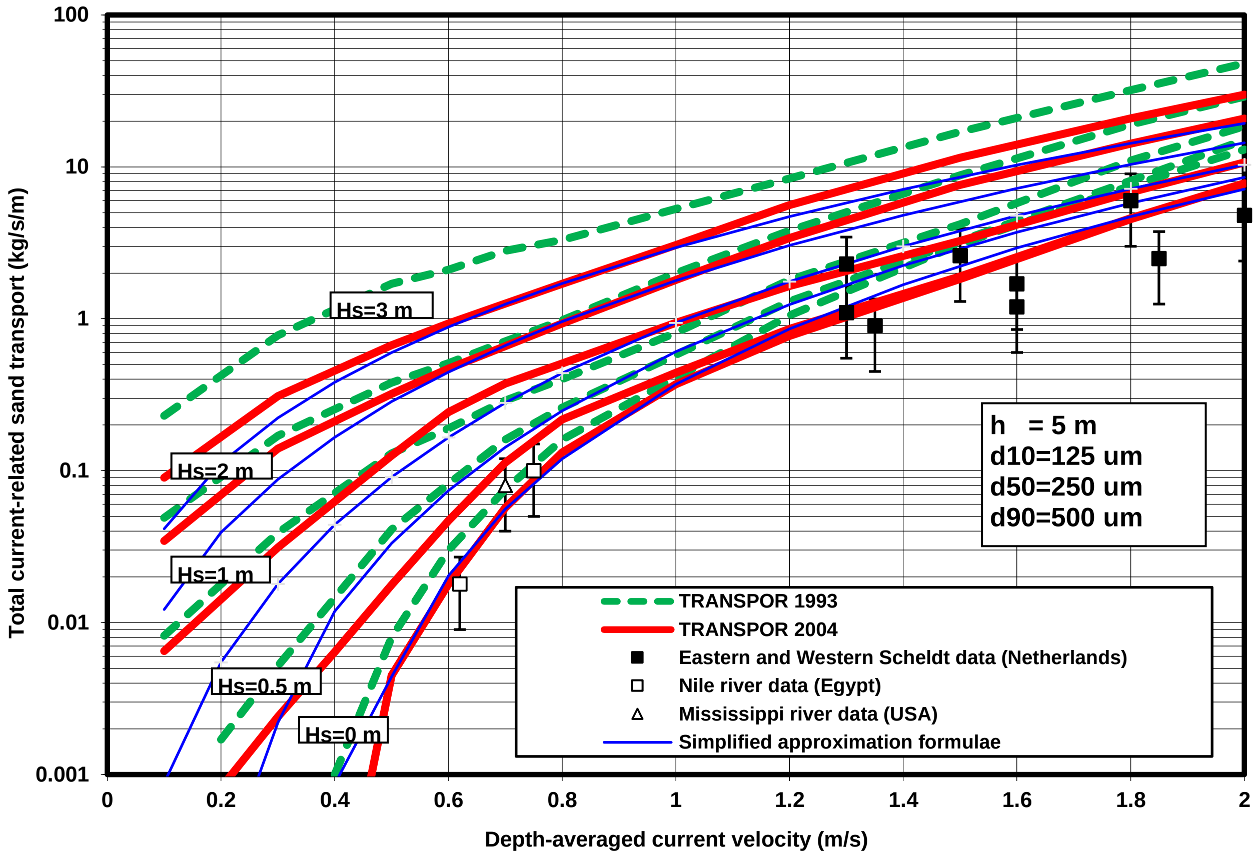

Figure 8 *Total sand transport for combined wave plus current conditions, h=5 m, d_{50}=250 μm.*

Depth h (m)	Velo city u (m/s)	Waves H_s (m) T_p (s)	Peak orbital velocity U_w (m/s)	Critcal velocity current $U_{cr,c}$ (m/s)	Critical velocity waves $U_{cr,w}$ (m/s)	Effective velocity U_e (m/s)	Computed bed load transport qb Eq. 6.2 (kg/s/m)	Computed suspended load transport q_s (kg/s/m) Eq. (6.3a)	 Eq. (6.3b)	 Eq. (6.4)
5	1	0	0	0.38	0	1	0.041	0.62	0.41	0.51
5	1	0.5; 5	0.26	0.38	0.17	1.10	0.057	1.02	0.68	0.71
5	1	1; 6	0.57	0.38	0.175	1.23	0.075	1.61	1.07	1.01
5	1	2; 7	1.21	0.38	0.185	1.48	0.115	3.09	2.06	1.77
5	1	3; 8	1.88	0.38	0.195	1.75	0.155	5.11	3.41	2.80

Angle current-wave direction φ= 90°; Temperature = 15° Celsius, Salinity= 0 promille; d_{50}=0.00025 m; d_{90}=0.0005 m

Table 2 *Computed sand transport rates*

7. References

Bagnold, R.A., 1956. *The Flow of Cohesionless Grains in Fluids. Proc. Royal Soc. Philos.Trans., London, Vol. 249.*

Bagnold, R.A., 1966. *An Approach to the Sediment Transport Problem from General Physics. Geological Survey Prof. Paper 422-I, Washington.*

Einstein, H.A., 1950. *The Bed-Load Function for Sediment Transportation in Open Channel Flow. Technical Bulletin No. 1026, U.S. Dep. of Agriculture, Washington, D.C.*

Engelund, F. and Hansen, E., 1967. *A Monograph on Sediment Transport in Alluvial Streams. Teknisk Forlag, Copenhagen, Denmark.*

Meyer-Peter, E. and Mueller, R., 1948. *Formulas for Bed-Load Transport. Sec. Int. IAHR congress, Stockholm, Sweden.*

Munk, W.H. and Anderson, E.R., 1948. *Notes on the theory of the thermocline. Journal of Marine Research, Vol. 3, p 276-295.*

Nikuradse, J., 1932. *Gesetzmässigkeiten der turbulente Strömung in glatten Rohren. Ver. Deut. Ing. Forschungsheft 356*

Shields, A., 1936. *Anwendung der Ähnlichkeitsmechanik und der Turbulenz Forschung auf die Geschiebebewegung. Mitt. der Preuss. Versuchsamst. für Wasserbau und Schiffbau, Heft 26, Berlin, Deutschland*

Soulsby, R., 1997. *Dynamics of marine sands. Thomas Telford, UK*

Van Rijn, L.C., 1984a. *Sediment Transport, Part I: Bed Load Transport. Journal of Hydraulic Engineering, ASCE, Vol. 110, No. 10.*

Van Rijn, L.C., 1984b. *Sediment Transport, Part II: Suspended Load Transport. Journal of Hydraulic Engineering, ASCE, Vol. 110, No. 11.*

Van Rijn, L.C., 1984c. *Sediment Transport, Part III: Bed Forms and Alluvial Roughness. Journal of Hydraulic Engineering, ASCE, Vol. 110, No. 12.*

Van Rijn, L.C., 1993, 2012. *Principles of sediment transport in rivers, estuaries and coastal seas. Aqua Publications, Amsterdam, The Netherlands (WWW.AQUAPUBLICATIONS.NL)*

Van Rijn, L.C., 2007. *Unified view of sediment transport by currents and waves, I: Initiation of motion, bed roughness, and bed-load transport. Journal of Hydraulic Engineering, 133(6), p 649-667.*

Van Rijn, L.C., 2007. *Unified view of sediment transport by currents and waves, II: Suspended transport. Journal of Hydraulic Engineering, 133(6), p 668-389.*